GLOBAL BIOGEOCHEMICAL CYCLES, VOL. 17, NO. 0, XXXX, doi:10.1029/2002GB001963, 2003

Amplifying effects of land-use change on future atmospheric CO_2 levels

Vincent Gitz
Centre International de Recherche sur l'Environment et le Développement-CNRS/EHESS, Nogent sur Marne, France

Philippe Ciais
Institut Pierre-Simon Laplace/Laboratoire des Sciences du Climat et de l'Environment-CEA, Gif sur Yvette, France

Received 22 July 2002; revised 2 October 2002; accepted 29 October 2002; published XX Month 2003.

[1] We constructed a model to analyze the interactions between land-use change and atmospheric CO_2 during the recent past and for the future. The primary impact of the conversion of forested lands to cultivated lands is to increase atmospheric CO_2, via losses of biomass and soil carbon to the atmosphere. This increase is likely to continue in the next decades, but its magnitude can vary according to each land-use scenario. We show that this first-order effect is further amplified by the correlated diminution of terrestrial sinks, because when croplands replace forests, the turnover time of excess carbon in the biosphere decreases, and hence the sink capacity of terrestrial ecosystems decreases. This effect acts to further increase by up to 100 ppm the CO_2 level reached by 2100, and it is of the same order of magnitude, although smaller, than climate-carbon feedbacks. Uncertainties on the magnitude of this land-use induced effect are large, because of uncertainties in the sink role of terrestrial ecosystems in the future and because of uncertainties inherent to the modeling of land-use induced carbon emissions. Such an extra rise in atmospheric CO_2 is however partially offset by the ocean reservoir and by sinks operating over undisturbed, pristine ecosystems, suggesting that conserving pristine forests with long turnover times might be efficient in mitigating the greenhouse effect. *INDEX TERMS:* 0315 Atmospheric Composition and Structure: Biosphere/atmosphere interactions; 1615 Global Change: Biogeochemical processes (4805); 0322 Atmospheric Composition and Structure: Constituent sources and sinks; *KEYWORDS:* land-use change, carbon cycle, future scenarios

Citation: Gitz, V., and P. Ciais, Amplifying effects of land-use change on future atmospheric CO_2 levels, *Global Biogeochem. Cycles*, *17*(0), XXXX, doi:10.1029/2002GB001963, 2003.

1. Introduction

[2] Land-use and land cover changes have been recognized to be responsible for a substantial part of anthropogenic greenhouse gases releases to the atmosphere. Of particular importance here is quantifying the impact of land-use changes on global atmospheric CO_2 levels both over the recent past and in the future. To do so, we have to examine how carbon flows between the different terrestrial pools when an ecosystem is disturbed in response to land-use activities. We also need to determine what is the fate of CO_2 emitted via land-use changes, in particular what fraction of it gets reabsorbed by the ocean, by undisturbed ecosystems, and remains in the atmosphere. Land-use changes have a myriad of socio-economic, and regional climatic impacts but we are only concerned here by their consequences on the perturbation of the carbon cycle. In contrast to fossil fuel emissions which are inventoried by energy statistics with an accuracy of about 10%, today's estimates of land-use induced carbon fluxes to the atmosphere are subject to large uncertainties [*Houghton et al.*, 2000]. First, there is an uncertainty on the area extent of land-use and land cover changes [*Houghton*, 1999; *Skole and Tucker*, 1993]. Second, there is an uncertainty in the amount of carbon that follows conversion from an ecosystem type to another, both for the amount of biomass that is released to the atmosphere as CO_2 during the conversion, but also for the delayed fluxes that follow the disturbance. This latter flux is associated to time constants of several years: When a forest is converted to cropland, for instance, carbon in the former forest soils gets released to atmosphere within on average 10 to 30 years [*Trumbore et al.*, 1995]. There is an even larger uncertainty on future projections of land-use induced CO_2 fluxes using models, because one has to first estimate the areas of loss or regrowth of ecosystems, and from there to compute the CO_2 losses to the atmosphere.

[3] Recent modeling studies using GCMs have highlighted positive carbon-climate feedbacks in the future, which result in an additionally higher CO_2 level by 80 to 200 ppm by 2100 in response to greenhouse warming [*Friedlingstein et al.*, 2001; *Dufresne et al.*, 2002; *Cox et*

0886-6236/03/2002GB001963$12.00

al., 2000]. Yet, those studies, as well as the current IPCC projections have treated land-use induced carbon fluxes identically as fossil fuel emissions, that is CO_2 is emitted from an inert reservoir into the atmosphere. Further, in the above studies, the vegetation cover was either assumed constant through time [*Dufresne et al.*, 2002] or evolving in response to climate [*Cox et al.*, 2000], but not in response to land-use. In reality, land-use consisting mainly of forest to cropland or forest to pasture conversion shortens the turnover of carbon above and below ground, and thus acts to reduce the sink capacity of the biosphere. Thus one may anticipate that coupling land-use emissions with a global carbon cycle description will yield to amplify future CO_2 levels as compared to the case where the global vegetation is considered as undisturbed.

[4] The aim of this paper is to quantify the impacts of past and future land-use changes on atmospheric CO_2 and on the associated changes in oceanic and biospheric pools. We constructed a model of the global carbon cycle, where land ecosystems and the ocean are treated in a simplified, aggregated manner, as in former studies [*Schimel et al.*, 1996; *Enting et al.*, 1994; *Wigley*, 1997]. The parameterization of the biosphere was derived from a more complex, spatially resolved model. The main originality of our model is that it calculates at each time step the flow of carbon within ecosystems following land-use disturbances, as well as the release of CO_2 into the atmosphere and its further redistribution between ocean, land and the atmosphere. Therefore, the model offers a description of the coupling between land-use changes and the global carbon cycle.

[5] We investigate the fact that deforestation causes a direct and indirect increase in atmospheric CO_2 levels, but that it may also enhance CO_2 absorption by "pristine," undisturbed forests, as well as by the ocean. Both effects are of opposite direction, but of different magnitudes. In the following, we provide a short description of our global carbon cycle model, and of its land-use flux module. We next force the model with prescribed fossil emissions and land-use area changes to compute the atmospheric CO_2 increase between 1700 and the present, which is compared with the observed rise. Finally, we compute future CO_2 trajectories for the four marker scenarios of the IPCC, and evaluate the impacts of land-use changes on the atmospheric CO_2 levels by 2100. A number of sensitivity tests are performed to the model key parameters, to draw some more general conclusions.

2. Methods

2.1. Carbon-Cycle Model Description

[6] Our global carbon cycle model consists of a reduced-form ocean model to quantify the ocean-atmosphere CO_2 exchange and of a terrestrial carbon cycle model to account for the fluxes between land and atmosphere. The terrestrial cycle integrates a detailed land-use module that allow for conversions of biomes, and calculates both the land-use related net CO_2 emissions following anthropogenic disturbances as well as the terrestrial uptakes over the remaining undisturbed ecosystems at each time step.

2.1.1. Ocean-Atmosphere Exchange

[7] We used mixed-layer ocean pulse response functions to represent the ocean-atmosphere exchange [*Joos et al.*, 1996]. The entire reduced form ocean model is described in Appendix A. We checked that our ocean model, for any given stabilization scenario, gives exactly the same results as the calculations of F. Joos (available at www.climate.unibe.ch).

2.1.1.1. Land Cover Map

[8] The global land cover in our model is based on a simplified vegetation map, which is regionalized into four world regions as defined by the Intergovernmental Panel of Climate Change Third Assessment Report (IPCC-TAR), and shown in Figure 1: OECD-1990 (North America, Europe, Japan and Australia), REF (Former Soviet Union and Eastern Europe), ASIA, ALM (Africa, Latin America and Middle East). In each region, six natural biomes are defined, plus three crop types (boreal, temperate, tropical) and cohorts of lands in transition between two biomes. Icy and hot desert were excluded. For each region, a biome has separate biophysical characteristics and it is assigned one surface area in the model. The regional preindustrial area extent of each biome is specified from the vegetation distribution used in the CASA-SLAVE biospheric model [*Friedlingstein*, 1995; *Friedlingstein et al.*, 1995], which served to parameter the terrestrial carbon cycle of our aggregated model.

2.1.2. Terrestrial Cycle

[9] On each biome j of each region k, of area $s_{j,k}$, we define a living vegetation reservoir, or biomass, $B_{j,k}(t)$ and a soil carbon reservoir $S_{j,k}(t)$. When there is no land-use change, the evolution of the biomass on a 1-year time step is given by

$$B_{j,k}(t+1) - B_{j,k}(t) = \eta_{j,k}(t) s_{j,k} - \mu_{j,k} B_{j,k}(t), \qquad (1)$$

where the biomass mortality is assumed to be a constant fraction $\mu_{j,k}$ of standing biomass and the net primary productivity $\eta_{j,k}$ is defined as a function of the atmospheric CO_2 concentration $C(t)$,

$$\eta_{j,k}(t) = \eta_{j,k}^{t=0}\left(1 + \beta \log \frac{C(t)}{C(0)}\right). \qquad (2)$$

When no land-use change happens, the dynamics of soil carbon is given by the following equation, where heterotrophic respiration is defined as a fraction of the soil carbon pool:

$$S_{j,k}(t+1) - S_{j,k}(t) = \mu_{j,k} B_{j,k}(t) - \delta_{j,k} S_{j,k}(t). \qquad (3)$$

In this study, temperature variations are not considered. Because we aim to evaluate individually the role of land-use, we assumed constant climate for simplicity, thus ignoring the response of heterotrophic respiration and NPP to temperature [*Cao and Woodward*, 1998; *Cramer et al.*, 2001].

[10] Three key parameters in our model, net primary productivity, biomass mortality and specific respiration rate, are derived, for each biome and region, from the spatially explicit CASA-SLAVE model. Those quantities are simply averaged from the CASA-SLAVE grid point values weighted by the area of each biome in each grid point.

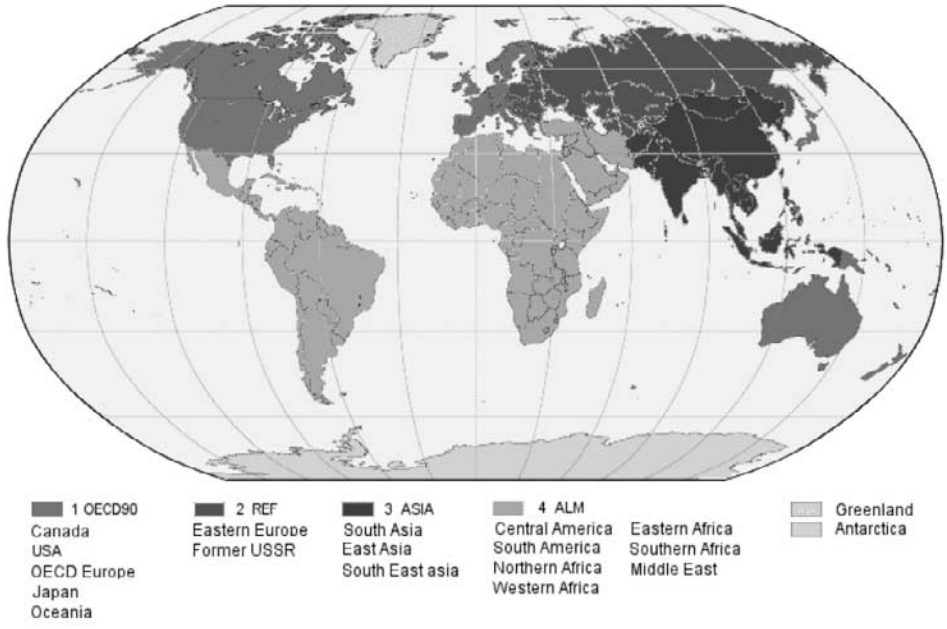

Figure 1. IPCC world regions.

We compared the preindustrial equilibrium stocks of our model to the CASA-SLAVE results (Appendix B). Overall, the aggregated model and the original CASA-SLAVE stocks agree with each other within better than 10% for each region and within 5% for global stocks. The largest relative difference (25%) between our model and CASA-SLAVE is obtained for the biomass of temperate grasslands and tundra, which nevertheless represents a very small pool. In terms of equilibrium fluxes, we calculated a global net primary productivity of 58 GtC/yr, very close to the one of CASA-SLAVE (61 GtC/yr). Despite its strong level of aggregation, given the equilibrium values in both models (Table 1), we are confident that our model is capable to compute changes in terrestrial pools that are comparable to the ones obtained with the more realistic and sophisticated CASA-SLAVE model.

2.1.3. Land-Use Module Description

[11] Each year, inside each region, deforestation causes an increase in crop area with time that is prescribed after *Houghton and Hackler* [2001] for the historical period. Conversion from forest to pasture is not included in our analysis, which likely implies an underestimate of our land-use source, especially in the tropics. We decided not to include this conversion type because of uncertainties on the fate of carbon in pastures linked to management issues (fodder grasses, animal load, pasture abandonment) that are difficult to address at our aggregated level. Also, future land-use change scenarios (see below) do not provide the conversion of forest to pasture. We made a test including conversion of forests to pastures as in the work by *Houghton and Hackler* [2001] over the historical period and obtained a global land-use emission that can be up to 30% higher than the one in Figure 2a.

[12] Conversely, agricultural abandonment reduces the grasslands area in favor of new forests. The land-use model is hence forced with annual area change data per biome and region. For the historical period, data published by *Houghton and Hackler* [2001] were lumped into our reduced biomes and regions definitions according to Table 1. We retained six major land-use transitions per region, encompassing forest to cropland conversion (deforestation) and grassland to forest conversion (afforestation), as shown in Table 1b. Logging

Table 1a. Correspondence Between Biomes in Our Model and in CASA-SLAVE

Model	CASA-SLAVE
Temperate forests	deciduous forests
Boreal forests	conifer forests
Tropical forests	tropical seasonal and evergreen forests
Temperate grasslands	C3 grasslands
Toundra	toundra
Tropical grasslands	C4 grasslands and savannas

Table 1b. Correspondence Between Conversions Between Biomes in Our Model and in Houghton

Model	Houghton (Appellation Depending on Region)
Temperate forests to temperate crops	temperate evergreen/deciduous/ broadleaf warm coniferous forest clearing for cropland
Temperate grasslands to temperate forests	temperate evergreen/deciduous forest afforestation or abandonment
Boreal forests to boreal crops	boreal forest clearing for cropland
Toundra to boreal forests	boreal forest abandonment
Tropical forests to tropical crops	tropical moist/open/closed/seasonal/ equatorial forest or woodland clearing for cropland
Tropical grasslands/savannas to tropical forests	tropical seasonal forest plantation

Table 1c. Correspondence Between Geographic Regions in Our Model and in Houghton

Model	Houghton
Model	Houghton
OECD 90	Canada, United States Europe, Pacific Developed Region,
ASIA	China, Mongolia South and Southeast Asia,
REF	Former Soviet Union,
ALM	South and Central America, North Africa Middle East, Tropical Africa.

and shifting cultivation present in Houghton's model are discarded here for simplicity, since being permanently offset by regrowth, they do not induce a large net flux to or from the atmosphere.

[13] The structure of our land-use module is similar to that of *Houghton* [1999] (that is, a book-keeping model that keeps track of ecosystems affected by land-use change) as well as carbon stocks and fluxes associated with them: This is done by defining cohorts of increasing age classes after each type of disturbance, up until some new "carbon equilibrium" is reached long after conversion (permanent crop or undisturbed forests). Here "carbon equilibrium" means zero net carbon flux in the absence of fertilization both in the vegetation and the soils. Details of this calculation are given in Appendix C.

[14] Following a forest conversion, a fraction of the standing biomass is lost to the atmosphere within 1 year, whereas the remaining harvested wood products are directed into two different reservoirs: a middle term reservoir of 10-year linear decay time and a long-term reservoir of 100-year linear decay time. The repartition coefficient varies with forest biomes and regions according to the specification given by *Houghton and Hackler* [2001]. Typically, after forest clearing, about 30% of the biomass goes into wood products pools.

[15] A newly converted land is assigned the specific NPP, mortality and heterotrophic respiration rates of the corresponding new biome. Eventually these values are different for transition cohorts according to their age. Net Primary Productivity of croplands was assigned the world average value determined by [*Goudriaan et al.*, 2001] from agricultural statistics (334 g/m^2/yr). We assumed that 70% of the annual crop biomass production is oxidized in the following year (harvest), and that the remaining 30% is delivered to the soil as litterfall.

[16] The soil respiration rates $\delta_{j,k}$ for croplands "active" soil pools was set equal to those of grasslands. According to equation (3) this quantity is the inverse of the turnover time of carbon in the soils. This gives a reasonable value of $\delta_{j,k}^{-1}$ for the crops, on the order of 10–20 years, in agreement with literature numbers [*Balesdent and Recous*, 1997; *Balesdent and Mariotti*, 1996; *Harrison et al.*, 1993].

2.2. Validation of the Model

2.2.1. Land-Use Module Validation

[17] Over the historical period, we compare in Figure 2 the Houghton land-use flux with our model response forced with land-use area changes at constant CO_2 concentration (280 ppm). We show here the results for the world, for temperate regions (OECD + REF) and for tropical regions (ASIA + ALM). Globally, the agreement is good between our simplified land-use module using the area changes of Houghton and the carbon parameters of CASA-SLAVE, and the original Houghton calculation. The two modeled land-use emissions in Figure 2a do not differ by more than 0.2 GtC/yr at any period of the interval 1700–1990. Such a difference is much smaller than current uncertainties on the land-use source reconstruction. On the other hand, our model systematically underestimates by 0.3 GtC/yr the land-use source to the atmosphere over temperate regions between 1700 and 1960, whereas it overestimates the source by approximately the same amount in the tropics as shown in Figures 2b and 2c.

[18] To explain such differences, it should be noted that biomes at equilibrium have different carbon content in the model of Houghton as compared to our model. Indeed, the use of CASA-SLAVE parameters gives in general a greater loss of carbon from soils after land-use change than specified by Houghton, whereas for biomass, the loss is smaller in our model than in that of Houghton. Soil carbon stocks are difficult to compare between Houghton's model and our model, as depth definitions are different. In the temperate region we calculate a higher release flux from soil carbon

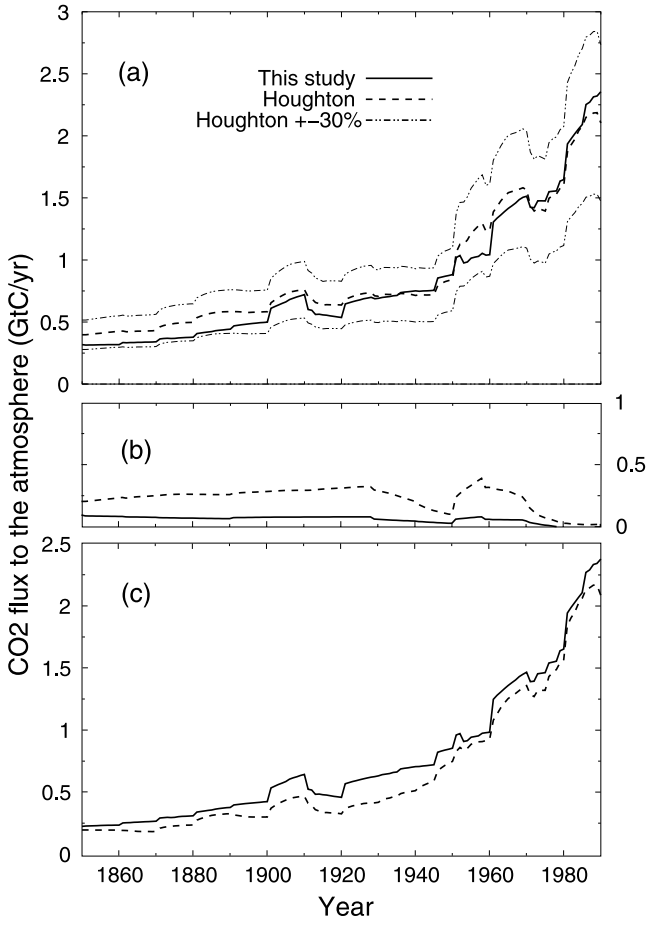

Figure 2. Historical net land-use CO_2 flux to the atmosphere in our model as compared to that of *Houghton and Hackler* [2001] for (a) global regions, (b) boreal and temperate regions, and (c) tropical regions.

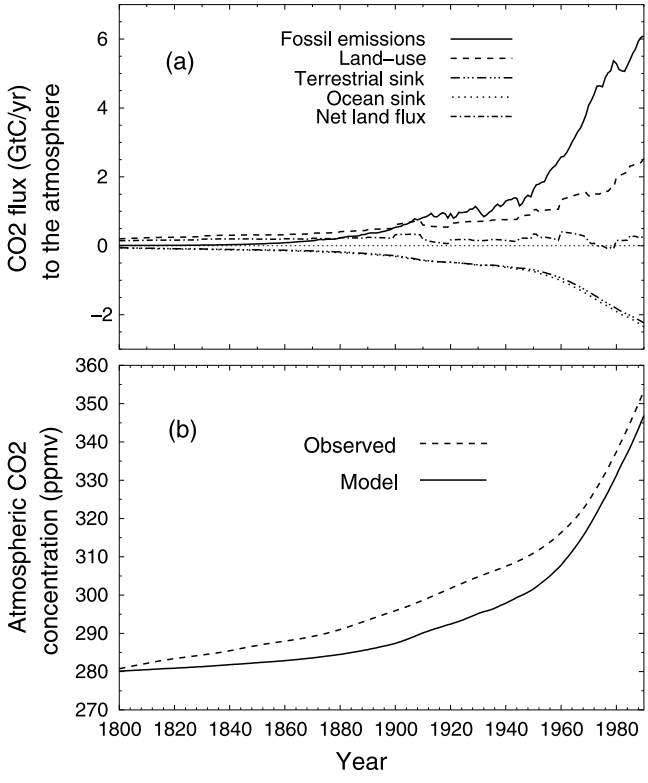

Figure 3. (a) Modeled historical changes in the carbon budget (by convention, sources are positive and sinks are negative) and (b) resulting atmospheric CO_2 concentration between 1800 and 1990.

due to land-use than in the Houghton model, but this effect is more than compensated by the fact that the biomass of temperate forests is higher in the Houghton model (13.5 kg/m^2) than in our model (7.4 kg/m^2), leading overall to a smaller emission curve as compared to Houghton's. In the tropics, forest biomass in the Houghton model (15 to 25 kg/m^2) is also higher than in our model (15 kg/m^2). This difference does not compensate for the discrepancy in the soil carbon stocks change, leading to slightly greater emissions in our model than in Houghton's for this region as shown in Figure 2c.

2.2.2. Components of the Historical Carbon Budget

[19] Over the period 1700–1990, we run the model forced with fossil CO_2 emissions and land-use areas change in ha/yr from Houghton. The model hence directly computes the net land-use source (Appendix C), the biospheric uptake due to time lag between increase of NPP and increase in heterotrophic respiration, the ocean sink (Appendix A) and the resulting atmospheric CO_2 concentration. Figure 3 shows all the components of the carbon budget through time and the pertaining atmospheric CO_2 curve.

[20] We calculate a rise in atmospheric CO_2 between the preindustrial period and the present (1980–2000) of 73.7 ppm, close to observed (75.4 ppm). This result corresponds to a β factor of 0.4 in equation (2), our control value of this parameter. The simulated rate of increase of CO_2 after 1970 is very close to the observation. It is, however, lower than observed between 1800 and 1970, yielding to an underestimate of the atmospheric CO_2 values by 10 ppm over that interval. It should be noted that using a single value of β tuned to match the contemporary budget proves generally difficult to reproduce the curvature of the atmospheric CO_2 history, as noted by [*Friedlingstein*, 1995; *Friedlingstein et al.*, 1995]. In addition to CO_2 fertilization, nitrogen deposition on ecosystems over industrialized continents, and variability in climate might contribute to modulate the uptake of carbon by the biosphere [*Cannell*, 1999]. Recent model runs by *McGuire et al.* [2001] indicate that the effects of climate trends and variability over the past century are unclear, and can result either in an extra source or in an extra sink of atmospheric CO_2 depending on which terrestrial biosphere model is used. Similarly, variability or shifts in the ocean circulation, not accounted for in our model, could be responsible for the mismatch. It remains also possible that both Houghton's and our calculation of the land-use source is underestimated over 1800–1970, as recent new estimations made by *Houghton* [2002] and *House et al.* [2001] suggest.

[21] Table 2 compares the carbon balance for the 1980s as resulting from the model and as estimated in the IPCC–TAR [*Prentice*, 2001]. In the period 1980–1989, the global ocean uptake is of 2.01 GtC/yr, in agreement with the IPCC-TAR estimates (Table 2).

[22] The biosphere is quasineutral (source of 0.21 GtC/yr), indicating that land-use emissions are approximately in balance with biospheric uptake elsewhere. This result is in agreement with the IPCC-TAR carbon budget for the 1980s but not for the 1990s where the biosphere is a much stronger net sink [*Prentice*, 2001]. In fact, the observed enhanced biospheric uptake in the 1990s reflects the impact of climate variability, in particular the cooling of Northern Hemisphere

Table 2. Average Carbon Budget for the 1980s and Cumulated Changes in Carbon Reservoirs in Our Model and in IPCC-TAR and IPCC-SRLULUCF Estimates[a]

	1980s Average Fluxes, GtC/yr		1850–1998 Cumulated Budget, GtC	
	Model	IPCC-TAR	Model	IPCC-SRLULUCF
Atmospheric increase	3, 24	3,3 ± 0.1	157	160
Fossil emissions	5, 45	5.4 ± 0.3	269	270 ± 30
Ocean uptake	−2, 01	−1,9 ± 0,6	−116	−120 ± 50
Land atmosphere flux partitioned as follows	0, 21	−0.2 ± 0.7	29	26 ± 60
Land-use emissions	2,22	1.7 (0.6 to 2.5)	139	136 ± 55
Terrestrial sink	−2,00	−1.9 (−3.8 to 0.3)	−110	−110 ± 80

[a]Convention: sources are positive and sinks are negative.

lands due to the climate effects of the eruption of Mount Pinatubo in 1991 [*Dutton and Christy*, 1992], an effect which is not present in our model. Regarding the cumulated stocks changes since the preindustrial times, our model gives values in very close agreement with those of the IPCC special report on LULUCF [*Bolin and Sukumar*, 2001] within their error bars, a result that is of course dependent on our setting of the β factor.

2.3. Land-Use Future Scenarios

[23] For the period 1990–2100 several integrated assessment models have been run in the IPCC Special Report on Emissions Scenarios (IPCC-SRES) to predict changes in land-use areas and CO_2 fluxes [*Nakicenovic et al.*, 2001]. We forced our model with both fossil-fuel emissions and land-use areas changes (in ha/yr), using data from the IMAGE 2.2 model IPCC-SRES scenarios A1F, A2, B1, B2, for the four considered world regions [*Bollen et al.*, 2001]. To be consistent with the historical period, we assumed that the loss in forest area yields to croplands, and that the gain in forest area occurs to the detriment of grasslands. Note that the IMAGE 2.2 scenarios already result from an integrated assessment approach, hence the variations in forest area might contain a part due to climate change. This part is likely marginal compared to anthropogenic land-use changes as evidenced by the correlated evolution of agricultural and forest biomes.

[24] Since the IMAGE 2.2 scenarios data used here do not distinguish between tropical, temperate, and boreal forest clearing within each region, we made the reasonable hypothesis that the ratio in the conversion of any pair of different types of biomes stays constant equal to the Houghton's historical average ratio. Note that there is an inconsistency in the total area that is modeled to be subject to land-use change by 1990 between Houghton and IMAGE 2.2. To overcome this problem, we apply only the rate of change in areas from IMAGE 2.2 to enter into the future after 1990, thus obtaining continuity from our historical curves. Given the IMAGE 2.2 land-use conversion estimates, we calculated forward future land-use areas using the initial 1990 areas as obtained in our model. On this basis, we can draw the CO_2 fluxes from and to all reservoirs in the fully interactive model up to 2100.

[25] The historical figures of land-use induced fluxes in IMAGE 2.2 are remarkably lower than those of Houghton. In the interval 1970–1990 for which there is an overlap in the two models, IMAGE 2.2 gives a land-use source of 1.06 GtC/yr, to be compared to 1.77 GtC/yr in the Houghton model for all land-use activities. This difference is even more surprising in that IMAGE 2.2 estimates a loss of forest area during 1970–1990 of 168 M ha, whereas Houghton gives 110 M ha, net of 40 M ha of afforestation. It thus seems that IMAGE 2.2, at comparable deforestation rates, produces a smaller land-use source than either Houghton or our model. For instance, in scenario A2, this feature is reflected in a land-use source of 3.6 GtC/yr by 2100 in our calculations, against 2.1 GtC/yr in IMAGE 2.2. It is in fact possible that IMAGE computes area changes over biomes whose characteristics (soil and biomass carbon stocks) are different than both in our model and in Houghton's. The difference is probably due to the fact that IMAGE's vegetation distribution is not based on observations or measures, but computed [*Alcamo et al.*, 1998].

3. Results

[26] Our modeling approach enables us to quantify the effects of land-use change on atmospheric CO_2 in the future and over the historical period. Primarily, just like for fossil fuel burning, the obvious impact of land-use change is to increase atmospheric CO_2, as implied by the loss of forest biomass and soil carbon when new croplands are established. Second, we show that an additional effect called here "land-use amplifier" yields an extra increase of CO_2 because land-use change also acts to diminish the sink capacity of the terrestrial biosphere by decreasing the residence time of carbon when croplands have replaced forests. Third, the extra increase of CO_2 gets limited because any additional increase of CO_2 resulting from the land-use amplifier effect stimulates the carbon uptake both by the oceans and by undisturbed ecosystems subject to CO_2 fertilization.

[27] In order to quantify the land-use amplifier effect, we carried out three simulations over the 1700–2100 period for each of the IPCC-SRES scenarios. The first experiment, called E1, is a standard model run where land-use induced CO_2 fluxes are computed interactively with the ocean and biospheric sinks, as driven by fossil fuel emissions and land-use area changes. Thus, E1 contains all the effects. The second experiment, called E2, inhibits the effect of reduced residence times as in E1. In E2, a land-use source identical to the one of E1 is injected into the atmosphere, with the terrestrial biosphere being kept to its preindustrial biome areas. In other words, in E2, the land-use source is treated as fossil fuel emissions, as done in former IPCC-TAR calculations. One can anticipate that, in experiment E2, the terrestrial biota is more efficient in absorbing CO_2 than in E1, so that in fine, the atmospheric CO_2 concentration level will be lower. The third experiment, called E3, disables the additional sinks created by the extra rise in CO_2 due to the interactive treatment of land-use in E1. In E3, land-use change occurs as in E1, but the ocean and the terrestrial biosphere "see" the atmospheric CO_2 trajectory computed in E2. One can anticipate that in E3 the atmospheric CO_2 level will be the highest of all.

[28] The E1-E2 difference accounts for the overall land-use amplifier magnitude: It shows how the E2 CO_2 concentration curve is modified when including land-use interactively. The E3-E2 difference shows how the E2 CO_2, calculated as in IPCC-TAR, would maximally underestimate the future atmospheric CO_2 level.

3.1. Land-Use Amplifier Effect for IPCC-SRES Scenario A2

[29] Here we analyze the effect for the IPCC-SRES scenario A2, with land-use change areas given by IMAGE 2.2 [*Bollen et al.*, 2001]. The A2 scenario reflects a future heterogeneous world with high regional disparities of income and high population growth in some regions, implying that natural resources are more depleted than in other IPCC-SRES scenarios [*Nakicenovic et al.*, 2001]. This scenario predicts a loss of forest area of 1180 M ha between

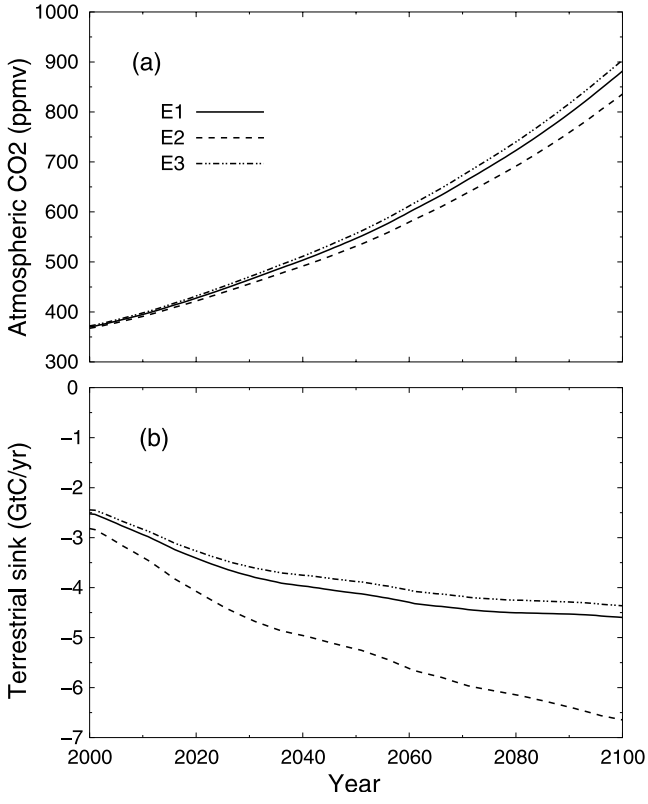

Figure 4. (a) Land-use effects on future atmospheric CO_2 levels. (b) Terrestrial sink over undisturbed ecosystems in experiments E1-E2-E3 under land-cover area changes and fossil fuel emissions from IPCC scenario A2.

1990 and 2100, to be compared with the 929 M ha already lost between 1700 and 1990 according to Houghton (this latter figure including conversions to pastures and shifting cultivation).

[30] It is seen in Figure 4 that for scenario A2, atmospheric CO_2 reaches up to 882 ppm by 2100 in the "standard" experiment E1. That is 46 ppm higher than in experiment E2 where land-use is treated as an "external source" such as fossil fuels and where the terrestrial biomes have preindustrial areas. On the other hand, in experiment E3, the atmospheric CO_2 by 2100 is higher than in E1 by 22 ppm.

3.1.1. Net Amplifier Effect

[31] The E1-E2 difference in Figure 4 is explained mostly by a less efficient biospheric sink in E1 where the carbon residence time is reduced over ecosystems affected by land-use change as compared to E2 where the biosphere state is preindustrial. The preindustrial global average residence time of carbon in the biosphere, in our model, is of 34.3 years. In experiment E1, by 2100, this value gets reduced to 30.0 years. Table 3 summarizes the partitioning of the carbon budget between atmosphere, ocean and the different biomes for all experiments. In terms of net fluxes, the difference E1-E2 is due to a weaker uptake of anthropogenic CO_2 in E1 (1.76 GtC/yr by 2100), partitioned into a reduced land uptake of 2.05 GtC/yr and an enhanced ocean uptake of 0.28 GtC/yr. In terms of cumulated fluxes, the positive net amplifier effect puts 98 GtC more carbon in the atmosphere. This value is the sum of 124.7 GtC not being absorbed into the biosphere and 27 extra GtC being absorbed by the ocean in E1 as compared to E2 as in Figure 4b. The relative difference (E1-E2)/E1 is equivalent to a 24% smaller global biospheric cumulated sink in E1, which represents 6.6% of the preindustrial stocks (see Table 3).

[32] In experiment E2, the relative proportion in the living biomass stock goes up from 36.0% in 1700 to 37.3% by 2100. This indicates that the sequestration of anthropogenic carbon is partitioned in the vegetation and in soils close to the preindustrial ratios. On the other hand, in experiment E1, the fraction sequestered in the vegetation diminishes to 32%, mainly because of the establishment of agricultural land instead of former forests, which does not allow for the formation of important biomass stocks. As expected, the ecosystems that benefit most of being fixed to their preindustrial area in E2 are tropical forests: Tropical forests alone accounts for 110 GtC of the enhanced biospheric cumulated uptake in E2 as compared to 22 GtC for temperate forests. Interestingly, boreal forests which remain quasi-undisturbed in the A2 scenario gain 3 GtC less carbon in E2. In other words, boreal forests are less efficient in E2 than in E1 to take up carbon simply because of lower atmospheric CO_2.

[33] In summary, over the period 1700–2100, the biosphere, sum of land-use sources and terrestrial sinks elsewhere, acts as a global net source in E1 (cumulated +22 GtC), and as a global net sink in E2 (cumulated −102 GtC). At face value, the ocean is more efficient in E1 (658 GtC sink) than in E2 (632 GtC sink). Thus, it can be seen that overall, the role of the biosphere explains most of the E1-E2 difference.

3.1.2. Maximal Amplifier Effect

[34] In E1, as compared to E2, the pristine terrestrial biosphere is being depleted, but the remaining part and the oceans, are however more stimulated by atmospheric CO_2. E3-E1 hence quantifies this "compensating" role of sinks in the net land-use amplifier effect. In E3, everything happens as in E1, except that the ocean and the terrestrial biosphere "see" the E2 atmospheric CO_2 concentration. So, in E3, the biosphere does not profit from the additional atmospheric CO_2 found in E1 due to interactive treatment of land-use. In terms of cumulated fluxes, this translates into 22.7 GtC less carbon sequestered on land in E3 as in E1. The oceanic uptake in E3 is equal to the one in E2 because of being calculated from the same CO_2 trajectory. E3-E2 gives the maximum value that land-use amplifier effects can induce. In terms of atmospheric CO_2, E3-E2 consists of 68 ppm by 2100, which implies that treating land-use as issued from an "external" reservoir such as fossil fuel emissions may underestimates the atmospheric CO_2 concentration by that amount, when the carbon cycle is operating at constant climate.

3.2. Comparison Among the Four IPCC-SRES Scenarios

[35] We now compare the land-use amplifier effect for the four different IPCC-SRES scenarios A1F, A2, B1, and B2, in Table 4. The emission scenarios are shown in Figure 5 together with our calculated land-use emissions. It is seen that A1F has the highest cumulated (1700–2100) fossil fuel

Table 3. Quantification of the Land-Use Amplifier Effect for IPCC Scenario A2 Using the Three Model Experiments Described in the Text[a]

	E1	E2	E3	E1-E2	E1-E3
Average Fluxes (GtC/yr) by 2100					
Atmospheric increase	18.77	17.01	19.25	1.77	−0.48
Fossil emissions	27.04	30.69	27.04	−3.64	0
Ocean Uptake	−7.08	−6.80	−6.80	−0.28	−0.28
Land atmosphere flux partitioned as follows	−0.96	−6.65	−0.75	5.69	−0.21
Land−use emissions	3.64	0	3.61	3.64	0.03
Terrestrial uptake partitioned as follows	−4.60	−6.65	−4.36	2.05	−0.23
Temperate forests	−1.45	−1.75	−1.37	+0.31	−0.07
Temperate grasslands	−0.27	−0.32	−0.26	+0.05	−0.01
Boreal forests	−0.87	−0.84	−0.83	−0.03	−0.04
Tundra	−0.11	−0.11	−0.11	−0.005	−0.01
Tropical Forests	−0.18	−2.00	−0.17	+1.81	−0.01
Tropical grasslands	−1.71	−1.63	−1.63	−0.08	−0.09
Cumulated Budget (GtC) 1700−2100					
Atmospheric increase	1282	1184	1328	98	−46
Fossil emissions	1936	2478	1936	−542	0
Ocean Uptake	−658	−632	− 632	−27	−27
Land atmosphere flux partitioned as follows	22	−645	44	668	−23
Land-use emissions	543	0	542	543	1
Terrestrial uptake partitioned as follows	−520	−645	−498	125	−22
Temperate forests	−146	−168	−140	+21.7	−6.5
Temperate grasslands	−28	−31	−26	+3.2	−3.9
Boreal forests	−85	−82	−81	−3.2	−3.0
Tundra	−10.2	−9.8	−9.8	−0.4	−1.2
Tropical Forests	−82	−193	−79	+110.5	−0.5
Tropical grasslands	−169	−162	−161	−7.1	−7.7

[a]In experiment E2, land-use emissions are treated identically to fossil fuel ones and therefore are included under the fossil emission totals.

emissions (2298 GtC) whereas B1 has the lowest ones (1212 GtC) by 2100. Regarding land-use, we calculate the highest cumulated source to the atmosphere using the A2 areas (543 GtC) and the lowest source using the B1 areas (62 GtC). In terms of atmospheric increase, the maximum level of atmospheric CO_2 is reached by 2100, ranging 500 ppm in B1 and 882 ppm in A2. Those numbers reflect primarily varying input of fossil fuel through time between 1700 and 2100 according to the different scenarios.

[36] The land-use induced net amplifier effect (E1-E2) on atmospheric CO_2 is the highest in A2 (46 ppm) and the lowest in B1 (13 ppm). The relative decrease in cumulated land uptake (E1-E2)/E1 varies between −12% and −24% among scenarios. The compensating role of sinks in the amplifier effect (E3-E1) is the highest in scenario A2 (22 ppm) and the lowest in B1 (15 ppm). This suggests that whatever the magnitude of the land-use source, large in A2 and small in B1, undisturbed ecosystems and the oceans always act to absorb a fraction of the additional atmospheric CO_2 present in E1 as compared to E2. This re-absorbed fraction is not negligible in comparison to the cumulated land-use source: 9% in A2 against 14% in B2, 34% in A1 and 51% in B1, showing the even importance of the role of sinks in "low intensity" scenarios. However, this important

Table 4. Cumulated Carbon Budget, Including the Land-Use Amplifier Effect, and Magnitude of the Amplification Effect for the Four IPCC Scenarios Considered

	A1	A2	B1	B2
Cumulated (GtC) 1700−2100 in Experiment E1				
Atmospheric CO_2 by 2100, ppm	842	882	500	609
Atmospheric increase	1197	1282	472	703
Fossil emissions	2298	1936	1212	1382
Ocean Uptake	−649	−658	−446	−527
Land atmosphere flux partitioned as follows	−440	22	−294	−148
Land-use emissions	117	543	62	271
Terrestrial uptake	−557	−520	−356	−420
Forest area change, 10^6 ha	25	−1909	413	−527
Land-Use Amplification on Atmospheric CO_2 (ppm) by 2100				
Difference E3-E2, ppm	51	68	28	40
Difference E3-E1, ppm	19	22	15	18
Net amplification E1-E2, ppm	32	46	13	22

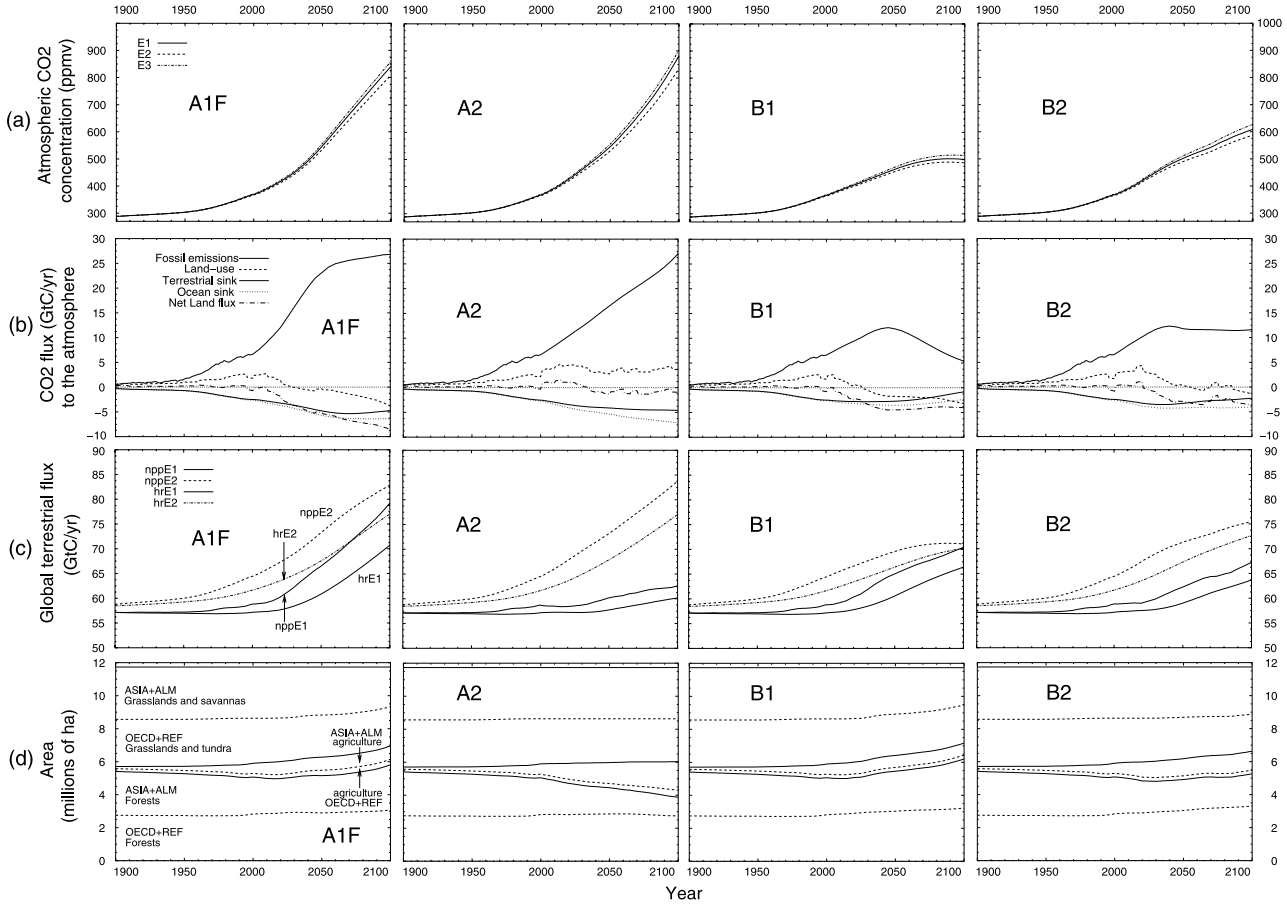

Figure 5. (a) Future atmospheric CO_2 trajectories with the land-use effects analyzed in experiments E1-E2-E3, for the four IPCC marker scenarios. (b) Pertinent emissions and ocean and land sinks. (c) Net primary productivity and heterotrophic respiration in E1 and E2. (d) Evolution of the areas of key biomes.

negative ''feedback'' might not exist in the future if the ocean and terrestrial sink were to be less efficient for other reasons (climate change, ocean circulation, etc.).

[37] All scenarios, except A2, have the peculiarity of stopping deforestation at around 2030 (Figure 5d), with land-use change inducing a net sink hereafter (Figure 5b). It should be noted that afforested lands are included within the land-use flux and not in the biospheric sink in Figure 5b. In all scenarios, the terrestrial sink over undisturbed ecosystems saturates by the end of the 21st century, and even diminishes, except in A2, as implied by a lower increase in atmospheric CO_2 (equations (1)–(3)). Under approximately the same atmospheric CO_2 trajectory as A2, scenario A1F has a land-use amplifier effect of 32 ppm which is quite important despite massive afforestation. Even if by 2100 under this scenario, forests have regained their 1700 extent, what determines the E1-E2 difference in this case is largely the destruction of forests that already took place in the past prior to 2100. In other words, in order for the land-use amplifier effect E1-E2 to be lowered by afforestation, this practice has to take place early enough so that a largest amount of carbon can be effectively sequestered into land ecosystems. It is also apparent in Figure 5a that there is a delayed effect in the E1-E2 difference, which appears by year 2000, after important land-use changes already happened and CO_2 rose significantly. The magnitude of E1-E2 is primarily dependent on the initial signal which is the rate of increase in atmospheric CO_2. It is only once atmospheric CO_2 has begun to rise significantly that it appears preferable for limiting the greenhouse effect to have maintained undisturbed forests (E2) rather than to have deforested them (E1). This advantage of preserving undisturbed forests might be conserved in the future as long as CO_2 continues to rise or as long as early afforestation is not implemented. In summary, among all scenarios, the land-use effects are sensitive first to the rate of increase of atmospheric CO_2, second to the initial state of the biosphere when atmospheric CO_2 begins to rise significantly, and third to future land-use scenarios which can either enlarge or inhibit the terrestrial sink.

[38] The fact that land-use change amplifies the atmospheric CO_2 concentration means that 1 GtC emitted via land-use contributes to atmospheric CO_2 increase more than 1 GtC of CO_2 emitted via fossil fuel burning. Table 5 quantifies this extra contribution of land-use change emissions to atmospheric CO_2 rise, that can be as high as 70% for A1. Inspection of the E1 and E2 experiment results for all scenarios further indicates that the airborne fraction,

Table 5. Atmospheric CO_2 Increase by 2100, in ppm, With Land-Use Amplifier Effects (E1) and Without Any Land-Use Change[a]

	A1	A2	B1	B2
Atmospheric CO_2 difference 2100–1700 (E1)	564	604	222	331
Atmospheric CO_2 difference 2100–1700 without land-use	518	423	212	261
Effective contribution of land-use change	46	181	11	70
"Fossil-equivalent" contribution of land-use change (E1)	27	132	10	54
Net amplifier effect E1-E2, ppm	32	46	13	22

[a]The "effective contribution of land-use change" is the difference between the two. "The fossil-equivalent" contribution of land-use change is equal to the atmospheric increase in E1 multiplied by the part of land-use emissions in the total anthropogenic emissions.

defined as the ratio of atmospheric increase to the cumulated fossil fuel emissions, is between 6 and 8% higher when the land-use effects are accounted for (E1) than when not (E2) in the considered scenarios. This effect would not show up in models, which consider the biosphere as undisturbed for its sink capacity, and by doing so treat land-use emissions such as fossil fuels. This shows the importance of an integrated approach to deal with land-use induced fluxes and the future CO_2 prediction.

3.3. Sensitivity Analysis to Key Parameters for Scenario A2

[39] As described by [*Thompson et al.*, 1996], we can characterize the biosphere response to an atmospheric CO_2 increase by mainly three parameters: the rate of increase of NPP with time, described here by a logarithmic β factor, the turnover time of carbon in the vegetation and soils, and the initial, preindustrial, NPP of the different biomes. We analyze below the sensitivity of the land-use carbon effects to each of the three above parameters. We take scenario A2 as an illustration. Figure 6 shows that the net amplifier effect E1-E2 increases with increasing preindustrial NPP and with increasing β. This is due to the fact that higher preindustrial NPP and higher β, or any combination of both, stimulate the sequestration by undisturbed ecosystems of an excess of carbon lost by land-use processes [*Kicklighter et al.*, 1999].

[40] Considering the role of global residence time, our model has a preindustrial global average turnover of 12.8 years in the vegetation and 21.5 years in the soils, yielding a 34.3 years average value. In order to change these turnover times of carbon in this sensitivity study independently of $NPP^{t=0}$, we varied the specific respiration rate δ and mortality rate μ in biomass in proportion of their preindustrial values. By doing so, we kept constant the ratio of turnovers in soils to the ones in vegetation but modified the global turnover of terrestrial carbon. Figures 6a and 6b show E1-E2 as a function of the triad global turnover time, β factor and preindustrial NPP. It is observed that when the turnover time increases, the immobilization of an excess carbon into the land biota lasts longer, and therefore a larger fraction of the land-use source gets reabsorbed within undisturbed ecosystems. The contribution of the ocean to the net land-use amplifier effect is contained in Figure 6 and is of opposite sign than the one of the biosphere, but we have shown in section 3.1.1 that the biosphere exerts a dominant control on the net effect.

4. Discussion

[41] In this work, only two mechanisms and their interactions are considered in controlling the role of the land biosphere on future CO_2 levels. Those two mechanisms are on the one hand CO_2 fertilization, which makes NPP increase in excess to respiration, and on the other hand the reduction of turnover times inducing a reduction in terrestrial sinks in response to deforestation. Those two effects oppose each other, and we have shown that significantly higher atmospheric CO_2 levels can be modeled by 2100 when land-use emissions are not treated as an external source such as fossil fuel use. This amplifying land-use

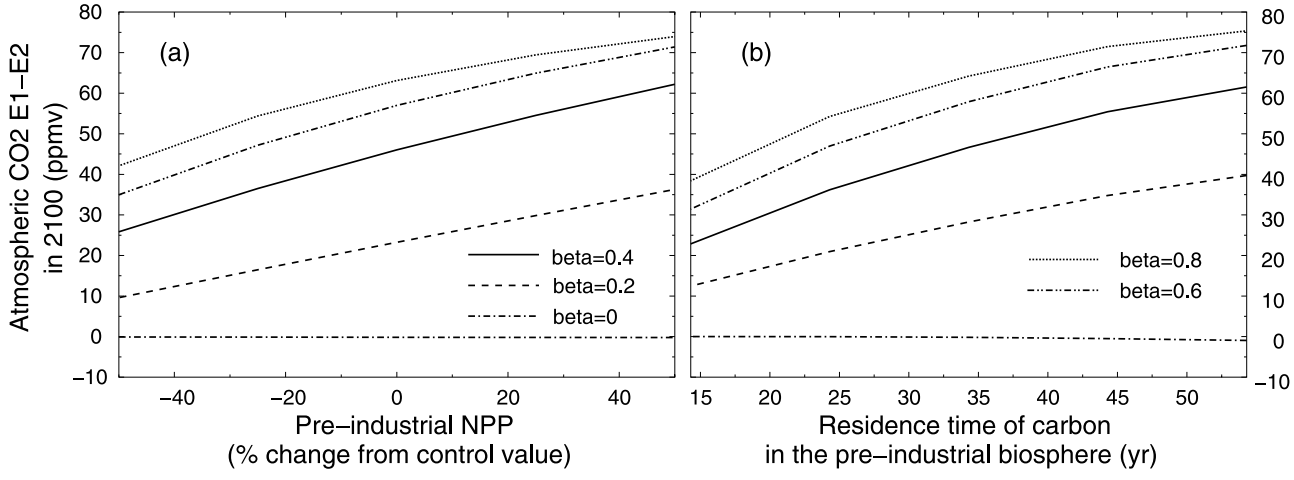

Figure 6. Amplifier effect defined by the difference in atmospheric CO_2 between E1 and E2 (a) to the β factor value versus the preindustrial NPP value. (b) Sensitivity to the β factor value and to the global turnover time of carbon on land.

Table 6. Atmospheric CO_2 by 2100 as a Function of the Fate of Harvested Wood Products Issued From Forest Conversion[a]

	Control Run (A2)	Long-Lived Wood Products	Short-Lived Wood Products
Atmospheric CO_2 by 2100, ppm	882	846	884
Difference E3-E2, ppm	68	66	68
Difference E3-E1, ppm	22	22	22
Amplification effect E1-E2, ppm	46	44	46

[a]In the ''long-lived'' case, wood products have a 100-year decay time against a 1-year decay time in the ''short-lived'' case. All numbers refer to the IPCC scenario A2.

effect depends on the parameters controlling the uptake of carbon on land: β, turnover, initial NPP, and on the emission scenario. It can be as high as 46 ppm additional CO_2 in the highest emission scenario. We have also shown that when atmospheric CO_2 increases in response to the conversion of forests to croplands, part of the resulting emissions end up being re-absorbed by oceans and by undisturbed ecosystems. If the remaining undisturbed tropical, temperate and boreal forests are still efficient in the future to take up CO_2, they will partly offset the effect of land-use changes in the tropics, but this ''land-use induced'' extra fertilization effect is probably limited (see Table 3, partitioning of the terrestrial uptake, last column E1-E3).

[42] In our model, a future ''translocation'' of carbon takes place between disturbed tropical pools and undisturbed pools elsewhere. At face value, if CO_2 fertilization is not as strong as previously thought over temperate and boreal forests [*Caspersen et al.*, 2000; *Schimel et al.*, 2000], or if the mechanisms responsible for the current biotic or oceanic sink happen to saturate in the future, then we will not benefit from this ''buffering'' of the land-use amplifier effect. In response, CO_2 will be even higher, and we estimated using the E3-E2 difference, that in such a ''worst case,'' atmospheric CO_2 can be 28 ppm (B1) to 68 ppm (A2) higher as compared to the current treatment of land-use in IPCC-TAR. For scenario A2, the uncertainty due to the model's parameters on the E3-E2 difference is on the order of $\pm$30 ppm. Thus, the uncertainty on the model's internal parameters is as high as the differences implied by various scenarios in estimating the land-use amplifier effect. It is worth noting that the land-use carbon amplifier effects are still lower in magnitude than the climate-carbon feedbacks estimated by coupled climate-carbon cycle studies [*Friedlingstein et al.*, 2001; *Dufresne et al.*, 2002; *Cox et al.*, 2000]. Integrated assessment models such as IMAGE may contain the effects that we found here, but they did not attempt to identify them separately and evaluate their magnitude.

[43] Associated with the loss of forests occurs a reduction of carbon turnover times in ecosystems. But there are also possibilities of managing the turnover of carbon affected by land-use change. Firstly, part of the biomass removed from forests is used in wood products pools of various decay times (see section 2.1.3) which in fine also are released as atmospheric CO_2. Thus, by managing the fate of wood products, humans can shorten or lengthen the turnover of terrestrial carbon, and consequently reduce or enlarge land-use effects. To check on this, we repeated E1 and E2 simulations assuming in a ''long-lived wood'' case that the wood products issued from deforestation after 1990 are piped into a 100-year linear decay pool and in a ''short-lived wood'' case that the harvested wood is all returned to the atmosphere within 1 year. In the ''long-lived'' test, atmospheric CO_2 in E1 is lower by 38 ppm than in the ''short-lived'' test (see Table 6). This indicates that the management of wood products coming from deforestation has potentially a large impact on atmospheric CO_2.

[44] A second management option concerns the establishment of croplands: The NPP of croplands is almost entirely manipulated by agricultural practices (fertilizer addition, species selection, irrigation, tillage, harvest of a large fraction of NPP which is not delivered to the soil) so that the impact of rising CO_2 alone on crop productivity might play only a minor role in increasing the carbon sinks over croplands. Future changes in agricultural practices might also contribute to enhance the turnover time of carbon in croplands. We tested a high and a low value for the residence time of cropland soil carbon: In the ''short'' case, this time is reduced from 20.8 (model average value) to 15.8 years, whereas in the long case we increased the time up to 35.8 years. A first obvious effect of increasing the residence time of carbon in croplands is to reduce substantially the land-use source following deforestation.

[45] However, the E1-E2 difference proves quite insensitive to the modifications of croplands' carbon turnover times, as shown in Table 7. The reason for this is that the E1-E2 difference is more sensitive to croplands' NPP^0 than to croplands' turnover times.

5. Conclusions

[46] We have constructed an aggregated carbon cycle model in order to study the interactions between land-use change and historical and future atmospheric CO_2 levels. This model is simpler than state-of-the-art, spatially explicit, terrestrial biosphere models because it encompasses only large regions of the world, with different biomes in each. It is however more detailed than the models that are used by the IPCC to evaluate future CO_2 levels: the treatment of land-use enables us to keep track of carbon lost during

Table 7. Atmospheric CO_2 by 2100 as a Function of Variations of the Average Residence Time of Carbon in Cropland Soils, for IPCC Scenario A2

	Short Case (15.8 years)	Long Case (35.8 years)
Atmospheric CO_2 by 2100 in E1, ppm	899	873
Land-use amplifier effect E1-E2, ppm	47.0	45.6
Cumulated Fluxes 1700–2100, GtC		
Land-use emissions (E1 and E2)	604	507
Terrestrial uptake (E1)	−531	−513
Terrestrial uptake (E2)	−658	−637
E1–E2 Difference in Terrestrial Uptake		
	−127	−124

forest conversion and of the resulting reduction of turnover times that it implies. We have shown that although the conversion of land cover change into carbon fluxes to the atmosphere remains highly uncertain, there is a net amplifying effect of land-use change on atmospheric CO_2. This net effect was unaccounted for in former IPCC assessments, and depends on the scenario of fossil fuel emission and of land cover changes, as well as on the model parameters controlling biospheric and oceanic uptake. It translates into 20 to 70 ppm higher CO_2 levels by 2100, of the same order of magnitude, but smaller than carbon-climate feedbacks obtained from GCM studies. This effect occurs because, in response to reduced turnover times over ecosystems subject to land-use, the global biosphere becomes progressively less and less efficient to absorb anthropogenic CO_2 in the future. At face value, undisturbed, pristine forests (and the ocean) act to stabilize this supplementary amplification of atmospheric CO_2, as their sink capacity increases when atmospheric CO_2 rises. These results suggest that there is a double benefit in keeping large stocks of forests in their pristine state, as far as those ecosystems are able to sequester atmospheric CO_2 [*Schulze et al.*, 2000]: It prevents the land-use source [*Schulze et al.*, 2002] and preserves the sink capacity of forested ecosystems. If carbon absorption of such pristine forests happens to saturate in the future, or is negatively affected by climate change, then the additional land-use amplifier effect alone would yield to an additional 100 ppm CO_2 at the end of the century (value obtained when the compensating role of sinks in the net effect vanishes). Efficient ''countermeasure'' to limit an increase in CO_2 pertaining to forest conversion would consist first in harvesting wood products when clearing forests, and increasing the lifetime of those products, and second in augmenting biomass export to the soil in croplands and/or residence times of carbon in cropland soils.

Appendix A: Description of the Air-Sea Flux Model

[47] We used the pulse function approach of *Joos et al.* [1996], for the HILDA model, at constant globally average surface temperature $T = 18.2°C$. Ocean-to atmosphere flux is computed by solving simultaneously equations (A1)–(A4). The notation Δ means that the variable is expressed as a difference to preindustrial state, where the atmospheric CO_2 concentration is C = 280 ppm. The change in total dissolved inorganic carbon, $\Delta\Sigma$ (in μC/kg), relative to preindustrial equilibrium in the ocean is given by

$$\Delta\Sigma = \frac{c}{h}\sum_{t'=t_0}^{t} f_{as}(t')r_s(t-t')dt', \tag{A1}$$

where h = 75 m is the depth of the ocean surface layer in meters and c is a conversion factor, $c = 1.722 \times 10^{17}\mu$mol/kg. The net air-sea flux per unit area $f_{as}(t)$ (in ppm $yr^{-1}m^{-2}$) is given by

$$f_{as}(t) = k_g(\Delta C - \Delta C_s), \tag{A2}$$

where $k_g = 1/9.06$ $yr^{-1}m^{-2}$ is a gas exchange coefficient, ΔC is the atmospheric CO_2 concentration and C_s is the surface ocean dissolved CO_2 concentration in ppm, the two latter quantities expressed by difference relative to preindustrial state. We used for $r_s(t)$ the HILDA model response functions,

$$\begin{aligned}
&\forall t \in [0,2]\\
r_s(t) = {}& 0.12935 + 0.21898\ exp(-t/0.034569)\\
&+0.17003\ exp(-t/0.26936)\\
&+0.24071\ exp(-t/0.96083)\\
&+0.24093\ exp(-t/4.9792)\\
&\forall t \in [2,+\infty]\\
r_s(t) = {}& 0.022936 + 0.24278\ exp(-t/1.2679)\\
&+0.13963\ exp(-t/5.2526)\\
&+0.089318\ exp(-t/18.601)\\
&+0.037820\ exp(-t/68.736)\\
&+0.035549\ exp(-t/232.30),
\end{aligned} \tag{A3}$$

We used the following calibration for the nonlinear chemical relationship between the perturbation in dissolved inorganic carbon and the concentration of CO_2 in surface waters:

$$\begin{aligned}
\Delta C_s = {}& (1.5568 - 1.3993\times10^{-2}T)\Delta\Sigma\\
&+(7.4706 - 0.20207T)\times10^{-3}(\Delta\Sigma)^2\\
&-(1.2748 - 0.12015T)\times10^{-5}(\Delta\Sigma)^3\\
&+(2.4491 - 0.12639T)\times10^{-7}(\Delta\Sigma)^4\\
&-(1.5468 - 0.15326T)\times10^{-10}(\Delta\Sigma)^5.
\end{aligned} \tag{A4}$$

Appendix B: Calibration of the Terrestrial Carbon Cycle Model

[48] Table B1 summarizes the parameters that were used over each region/biome from the CASA-SLAVE model and the resulting preindustrial biomass and soils carbon stocks.

Appendix C: Analytical Description of the Land-Use Change Bookkeeping Model

[49] Each IPCC region k = 1..4 is divided into three climatic zones l = 1..3. Land-use transitions between equilibrium biomes occur within each (k, l) subregion. In each subregion (k, l), the land-use bookkeeping model has the same structure described here. Age-classes for surfaces in transition between equilibrium biomes are defined, representing the time τ in years for an ecosystem to reach the new equilibrium state. Let τ_d be the recovery time for the deforestation transition, from undisturbed forests (F, u) to established crops (A, u). Let τ_r be the recovery time following reforestation, from grasslands (G) to recovered forests (F, u). Carbon equilibrium is defined for a balanced between input and output in absence of any mechanism that creates an increase in NPP.

[50] Let $s_{X,i}$ be the surface of biome X = F, A, G in age class i = 1, ..τ.., u. $def(t)$ is annual deforestation in hectares, $ref(t)$ is reforestation (prescribed in the (k, l) subregion). In the time period between t and $t+1$, the evolution of forests area is given by

$$\begin{aligned}
&S_{F,1}(t+1) = ref(t)\\
&\forall\tau \in [2,\tau_r], s_{F,\tau}(t+1) = s_{F,\tau-1}(t)\\
&s_{F,u}(t+1) = s_{F,u}(t) + s_{F,\tau_r}(t) - def(t).
\end{aligned} \tag{C1}$$

Table B1. Specific CASA-SLAVE Parameters Averaged Over Each Region That are Used in Our Model[a]

	Parameters				Results, GtC			
					Biomass		Soils	
Region	Area, 10^6 ha	$NPP^{t=0}$, g/m^2/yr	$\mu^{t=0}$, %/yr	$\delta^{t=0}$, %/yr	CS	Model	CS	Model
			Temperate Forests Biome					
OECD	600	593	7.47	5.16	48	44	69	69
REF	212	451	11.25	5.79	8	8	17	16
ASIA	408	671	5.92	4.15	46	44	66	63
ALM	625	1000	5.75	3.88	109	102	161	155
World	1845	732	6.40	4.32	211	197	312	302
			Boreal Forests Biome					
OECD	778	460	9.38	5.18	38	35	69	65
REF	1249	275	14.69	6.83	23	20	50	47
ASIA	11 4	829	5.90	3.26	16	15	29	28
ALM	61	564	3.51	2.08	10	9	17	17
World	2201	377	9.50	5.04	87	79	165	157
			Tropical Forests Biome					
OECD	52	884	12.84	9.42	4	4	5	2
ASIA	455	884	6.05	5.25	67	62	77	73
ALM	1127	1000	6.09	4.38	185	174	257	243
World	1634	964	6.18	4.65	255	239	339	318
			Temperate Grasslands Biome					
OECD	511	266	33.99	4.44	4	3	31	29
REF	722	98	10.66	2.31	7	6	31	30
ASIA	513	221	38.69	4.96	3	2	23	22
World	1746	183	23.57	3.81	14	10	84	81
			Tundra Biome					
OECD	513	58	6.92	1.57	4	4	19	18
REF	514	83	30.17	6.27	1	1	7	6
ASIA	43	305	21.81	3.60	1	1	4	4
World	1070	80	13.50	2.90	6.3	6	30	28
			Tropical Grasslands Biome					
OECD	625	253	37.20	15.39	4	10	10	9
ASIA	309	519	8.89	4.40	18	9	37	35
ALM	2308	570	9.13	4.84	144	121	272	259
World	3242	504	9.82	5.13	166	165	319	302
			All Biomes					
World	11738	494	7.83	4.64	740	697	1248	1188

[a] $NPP^{t=0}$ is the net primary productivity, $\mu^{t=0}$ is the biomass mortality and $\delta^{t=0}$ is the soil respiration rate for preindustrial conditions.

The evolution of cropland area is given by

$$\begin{aligned} rcls_{A,1}(t+1) &= def(t) \\ \forall \tau \in [2,\tau_d], s_{A,\tau}(t+1) &= s_{A,\tau-1}(t) \\ s_{A,u}(t+1) &= s_{A,u}(t) + s_{A,\tau_d}(t). \end{aligned} \tag{C2}$$

The evolution of grassland area is given by

$$s_G(t+1) = s_G(t) - ref(t) \tag{C3}$$

On each surface $s_{X,i}$, equations (C4)–(C6), state for the evolution of biomass $B_{X,i}(t)$, following land-use change and regrowth/mortality during the $[t, t+1]$ period. The net primary productivity $\eta(C)$ is given by equation (2). For forests,

$$\begin{aligned} B_{F,1}(t+1) &= \big(\eta_{F,1}(C) ref(t)\big)(1-\mu_F) \\ \forall \tau \in [2,\tau_r], B_{F,\tau}(t+1) &= \big(B_{F,\tau-1}(t) \\ &+ \eta_{F,\tau}(C) s_{F,\tau}(t+1)\big)(1-\mu_F) \\ B_{F,u}(t+1) &= \left(B_{F,\tau_r}(t) + B_{F,u}(t)\left(1 - \frac{def(t)}{s_{F,u}(t)}\right)\right. \\ &\left. + \eta_{F,u}(C) s_{F,u}(t+1)\right)(1-\mu_F); \end{aligned} \tag{C4}$$

for cropland,

$$\begin{aligned} B_{A,1}(t+1) &= \big(\eta_{A,1}(C) def(t)\big)(1-\mu_A) \\ \forall \tau \in [2,\tau_d], B_{A,\tau}(t+1) &= \big(B_{A,\tau-1}(t) + \eta_{A,\tau}(C) s_{A,\tau}(t+1)\big)(1-\mu_A) \\ B_{A,u}(t+1) &= \big(B_{A,u}(t) + \eta_{A,\tau}(C) s_{A,\tau_d}(t+1)\big)(1-\mu_A); \end{aligned} \tag{C5}$$

for grasslands,

$$B_G(t+1) = \left(B_G(t)\left(1 - \frac{ref(t)}{s_G(t)}\right) + \eta_G(C) s_G(t+1)\right)(1-\mu_G), \tag{C6}$$

where μ_X is the biome specific mortality rate, $\eta_{X,i}(C)$ is the biome specific net primary productivity function of the atmospheric CO_2 concentration C (equation (2)). In summary, the changing vegetation "sticks to" the surface rotation, except for deforestation, and grows and dies according to NPP and mortality.

[51] The soil carbon content $S_{X,i}(t)$ also strictly follows the surface rotation. Given the soil specific respiration rate $\delta_{X,i}$, the evolution of soil carbon after a change in land cover is given by the following equations for forests:

$$\begin{aligned}
S_{F,1}(t+1) &= \left(S_G(t)\frac{ref(t)}{s_G(t)} + \mu_F \eta_{F,1}(C) ref(t)\right) \\
&\quad \cdot\left(1-\delta_{F,1}\right) \\
\forall \tau \in [2,\tau_r], S_{F,\tau}(t+1) &= \left(S_{F,\tau-1}(t)\right. \\
&\quad \left.+\mu_{F,\tau}\eta_{F,\tau}(C)s_{F,\tau}(t+1)\right)\left(1-\delta_{F,\tau}\right) \\
S_{F,u}(t+1) &= \left(S_{F,\tau}(t) + S_{F,u}(t)\left(1-\frac{def(t)}{s_{F,u}(t)}\right)\right. \\
&\quad \left.+\mu_{F,u}\eta_{F,u}(C)s_{F,u}(t+1)\right)\left(1-\delta_{F,u}\right);
\end{aligned} \tag{C7}$$

for cropland:

$$\begin{aligned}
S_{A,1}(t+1) &= \left(S_{A,u}(t)\frac{ref(t)}{s_{A,u}(t)}\mu_A\eta_{A,1}(C) def(t)\right) \\
&\quad \cdot\left(1-\delta_{A,1}\right) \\
\forall \tau \in [2,\tau_d], S_{A,\tau}(t+1) &= \left(S_{A,\tau-1}(t)\right. \\
&\quad \left.+\mu_A\eta_{A,\tau}(C)s_{A,\tau}(t+1)\right)\left(1-\delta_{A,\tau}\right) \\
S_{A,u}(t+1) &= \left(S_{A,u}(t) + S_{A,\tau_d}(t)\right. \\
&\quad \left.+\mu_A\eta_{A,\tau_d}(C)s_{A,\tau_d}(t+1)\right)\left(1-\delta_{A,u}\right);
\end{aligned} \tag{C8}$$

for grasslands:

$$\begin{aligned}
S_G(t+1) &= \left(S_G(t)\left(1-\frac{ref(t)}{s_G(t)}\right)\right. \\
&\quad \left.+\mu_G\eta_G(C)s_G(t+1)\right)(1-\delta_G),
\end{aligned} \tag{C9}$$

where $\delta_{X,i}$ is the soil specific respiration rate. Each year, over each subregion, we have an immediate $f_i(t)$ land-use source to the atmosphere, encompassing the destruction of biomass,

$$f_i(t) = B_G(t)\frac{ref(t)}{s_G(t)} + (1-\omega)B_{F,u}(t)\frac{def(t)}{s_{F,u}(t)}, \tag{C10}$$

where ω is the part of the forest biomass that is harvested during land-use change and directed into the wood products pool. Each year, there is also a delayed land-use source $f_d(t)$, which concerns lands in transition to a new biome plus already established croplands, as well as decaying wood products: Here $f_d(t)$ is the difference between NPP and HR fluxes on those lands, plus the flux to the atmosphere coming out of the wood products pool, $f_{wp}(t)$.

$$\begin{aligned}
f_d(t) = &\sum_{\tau=1..\tau_r}\left(S_{F,\tau}(t)\delta_{F,\tau} - \eta_{F,\tau}(C)s_{F,\tau}(t)\right) \\
&+\sum_{\tau=1..\tau_d,u}\left(S_{A,\tau}(t)\delta_{A,\tau} - \eta_{A,\tau}(C)s_{A,\tau}(t)\right) + f_{wp}(t).
\end{aligned} \tag{C11}$$

Finally, the biospheric uptake due to CO_2 fertilization affecting undisturbed forests and undisturbed grasslands is given by $f_{au}(t)$,

$$f_{au}(t) = s_{F,u}(t)\eta_{F,u}(C) - \delta_{F,u}S_{F,u}(t) + s_G(t)\eta_G(C) - \delta_G S_G(t). \tag{C12}$$

Overall, the evolution of atmospheric CO_2 between t and $t+1$ (1 year), is given by

$$\begin{aligned}
C(t+1) - C(t) = &E(t) - s_{oc}f_{as}(t) \\
&+\sum_{k=1}^{4}\sum_{l=1}^{3}\left(f_i^{k,l}(t) + f_d^{k,l}(t) - f_{au}^{k,l}(t)\right),
\end{aligned} \tag{C13}$$

where $E(t)$ are the global fossil CO_2 emissions in year t, $s_{oc} = 3.62 \times 10^{14}\mathrm{m}^2$ is the ocean's area, and f_{as} is the net air-sea flux per unit area (equations (A1)–(A4)) in year t.

References

Alcamo, J., E. Kreileman, M. Krol, R. Leemans, J. Bollen, J. van Minnen, M. Schaeffer, S. Toet, and B. de Vries, Global modelling of environmental change: An overview of IMAGE 2.1, Appendix D: The terrestrial vegetation model, in *Global Change Scenarios of the 21stCentury*, edited by J. Alcamo, R. Leemans, and E. Kreileman, pp. 71–82, Pergamon, New York, 1998.

Balesdent, J., and A. Mariotti, Measurement of soil organic matter turnover using 13C natural abundances, in *Mass Spectrometry of Soils*, edited by T. W. Boutton and S. I. Yamasaki, pp. 83–111, Marcel Dekker, New York, 1996.

Balesdent, J., and S. Recous, Les temps de residence du carbone et le potentiel de stockage de carbone dans quelques sols cultives francais, *Can. J. Soil Sci.*, *77*, 187–193, 1997.

Bolin, B., and R. Sukumar, Global perspective, in *IPCC Special Report Land-Use, Land-Use Change and Forestry*, edited by R. T. Watson et al., pp. 23–51, Cambridge Univ. Press, New York, 2001.

Bollen, J., et al., The IMAGE 2.2 implementation of the SRES scenarios: A comprehensive analysis of emissions, climate change and impacts in the 21st century [CD-ROM], *Publ. 481508018*, Natl. Inst. of Public Health and the Environ., Bilthoven, Netherlands, 2001.

Cannell, M., Relative importance of increasing atmospheric CO_2, N deposition and temperature in promoting european forest growth, in *Causes and Consequences of Accelerating Tree Growth in Europe, EFI Proc.*, *vol. 27*, edited by T. Karjalainen, H. Spiecker, and O. Laroussiniepp, pp. 25–42, Eur. For. Inst., Joensuu, Finland, 1999.

Cao, M., and F. Woodward, Dynamic responses of terrestrial ecosystem carbon cycling to global climate change, *Nature*, *393*, 249–252, 1998.

Caspersen, J. P., S. W. Pacala, J. C. Jenkins, G. C. Hurtt, P. R. Moorcroft, and R. A. Birdsey, Contributions of land-use history to carbon accumulation in U. S. forests, *Science*, *290*, 1148–1151, 2000.

Cox, P. M., R. A. Betts, C. D. Jones, S. A. Spall, and I. J. Totterdell, Acceleration of global warming due to carbon-cycle feedbacks in a coupled climate model, *Nature*, *408*, 184–187, 2000.

Cramer, W., et al., Global response of terrestrial ecosystem structure and function to CO_2 and climate change: Results from six dynamic global vegetation models, *Global Change Biol.*, *7*, 357–373, 2001.

Dufresne, J., P. Friedlingstein, P. Cox, and P. Rayner, On the magnitude of positive feedback between climate change and the carbon cycle, *Geophys. Res. Lett.*, 292002.

Dutton, E. G., and J. R. Christy, Solar radiative forcing at selected locations and evidence for global lower tropospheric cooling the eruption of El Chichon and Pinatubo, *Geophys. Res. Lett.*, *19*, 2313–2316, 1992.

Enting, I., T. Wigley, and M. Heimann, Future emissions and concentrations of carbon dioxide: Key ocean/atmosphere/land analyses, *CSIRO Div. Atmos. Res. Tech. Pap. 31*, Commonwealth Sci. and Indust. Res. Org., Melbourne, Victoria, Australia, 1994.

Friedlingstein, P., Modelisation du cycle du carbone biospherique et etude du couplage biosphere-atmosphere, Ph.D. thesis., Inst. d'aeron. spatiale de Belgique, Brussels, Belgium, 1995.

Friedlingstein, P., I. Fung, E. Holland, J. John, G. Brasseur, D. Erickson, and D. Schimel, On the contribution of CO_2 fertilization to the missing biospheric sink, *Global Biogeochem. Cycles*, *9*, 541–556, 1995.

Friedlingstein, P., L. Bopp, P. Ciais, J.-L. Dufresne, L. Fairhead, H. Le-Treut, P. Monfray, and J. Orr, Positive feedback between future climate change and the carbon cycle, *Geophys. Res. Lett.*, *28*, 1543–1546, 2001.

Goudriaan, J., J. R. Goot, and P. W. Uithol, Productivity of agro-ecosystems, in *Terrestrial Global Productivity*, edited by J. Roy, B. Saugier, and H. A. Mooney, Academic, San Diego, Calif., 2001.

Harrison, K. G., W. S. Broecker, and G. Bonani, The effect of changing land-use on soil radiocarbon, *Science*, *262*, 725–726, 1993.

Houghton, R., The annual net flux of carbon to the atmosphere from changes in land-use 1850–1990, *Tellus, Ser. B*, *50*, 298–313, 1999.

Houghton, R., Revised estimates of the annual net flux of carbon to the atmosphere from changes in land-use and land management, *Tellus*, in press, 2002.

Houghton, R., and J. Hackler, Carbon flux to the atmosphere from land-use change, technical report, Carbon Dioxide Inf. Anal. Cent., Oak Ridge, Tenn., 2001. (Electronic data available at http://cdiac.esd.ornl.gov/ndps/ndp050.html)

Houghton, R., D. Skole, C. A. Nobre, J. L. Hackler, K. T. Lawrence, and W. H. Chomentowski, Annual fluxes of carbon from deforestation and regrowth in the brazilian Amazon, *Nature*, *403*, 301–304, 2000.

House, J., I. Prentice, M. Heimann, and R. Houghton, Uncertainties in the global terrestrial CO_2 sink, paper presented at 6th International CO_2-Conference, Tohoku Univ., Sendai, Japan, 2001.

Joos, F., M. Bruno, R. Fink, U. Siegenthaler, T. F. Stocker, C. L. Quere, and J. L. Sarmiento, An efficient and accurate representation of complex oceanic and biospheric models of anthropogenic carbon uptake, *Tellus, Ser. B*, *48*, 397–417, 1996.

Kicklighter, D. W., et al., A first-order analysis of the potential role of CO_2 fertilization to affect the global carbon budget: A comparison of four terrestrial biosphere models, *Tellus, Ser. B*, *51*, 343–366, 1999.

McGuire, A. D., et al., Carbon balance of the terrestrial biosphere in the twentieth century: Analyses of CO_2, climate and land-use effects with four process-based ecosystem models, *Global Biogeochem. Cycles*, *15*, 183–206, 2001.

Nakicenovic, N., et al., An overview of scenarios, in *IPCC Special Report on Emissions Scenarios*, edited by N. Nakicenovic and R. Swart, pp. 5–10, Cambridge Univ. Press, New York, 2001.

Prentice, I., The carbon cycle and atmospheric carbon dioxide, in *IPCC Third Scientific Assessment Report of Climate Change*, edited by J. T. Houghton et al., pp. 183–237, Cambridge Univ. Press, New York, 2001.

Schimel, D., D. Alves, I. Enting, M. Heimann, F. Joos, D. Raynaud, and T. Wigley, CO_2 and the global carbon cycle, in *Climate Change 1995: The Science of Climate Change, Contribution of WGI to the Second Assessment Report of the IPCC*, edited by J. T. Houghton et al., pp. 76–86, Cambridge Univ. Press, New York, 1996.

Schimel, D., et al., Contribution of increasing CO_2 and climate to carbon storage by ecosystems in the United States, *Science*, *287*, 2004–2006, 2000.

Schulze, E.-D., C. Wirth, and M. Heimann, Managing forests after Kyoto, *Science*, *289*, 20582000.

Schulze, E.-D., R. Valentini, and M.-J. Sanz, The long way from Kyoto to Marrakesh: Implications of the Kyoto Protocol negotiations for global ecology, *Global Change Biol.*, *8*, 505–518, 2002.

Skole, D., and C. Tucker, Tropical deforestation and habitat fragmentation in the Amazon: Satellite data from 1978 to 1988, *Science*, *260*, 1905–1910, 1993.

Thompson, M. V., J. T. Randerson, C. M. Malmstrom, and C. B. Field, Change in net primary production and heterotrophic respiration: How much is necessary to sustain the terrestrial carbon sink?, *Global Biogeochem. Cycles*, *10*, 726–771, 1996.

Trumbore, S. E., E. A. Davidson, P. B. de Camargo, D. C. Nepstad, and L. A. Martinelli, Belowground cycling of carbon in forests and pastures of eastern Amazonia, *Global Biogeochem. Cycles*, *9*, 515–528, 1995.

Wigley, T. M. L., Implications of recent CO_2 emission-limitation proposals for stabilization of atmospheric CO_2 concentrations, *Nature*, *390*, 267–270, 1997.

P. Ciais, Institut Pierre-Simon Laplace/Laboratoire des Sciences du Climat et de l'Environment-CEA, Saclay, 91191, Gif sur Yvette, France. (ciais@lsce.saclay.cea.fr)

V. Gitz, Centre International de Recherche sur l'Environment et le Développement-CNRS/EHESS, 45 bis avenue de la Belle Gabrielle, 94736Nogent sur Marne, France. (gitz@centre-cired.fr)